

## EMPIRICAL ESTIMATION OF HEAVY GOODS VEHICLE TYRE WEAR



J. Lepine\*  
Research Associate,  
University of  
Cambridge, UK  
Obtained his PhD from  
Victoria University in  
Australia in 2017.



S. Burgess  
MEng student at the  
University of  
Cambridge, UK,  
graduating in 2018



D. Cebon  
Professor of  
mechanical  
engineering at the  
University of  
Cambridge.  
Received his PhD from  
University of  
Cambridge, UK, in  
1985.

### Abstract

This paper presents an empirical estimation of heavy goods vehicle tyre wear as a function of slip angles, based on a model derived from experimental measurements. A novel technique was developed to measure tyre wear using a semi-trailer equipped with an active steering system. The trailer steering system enabled recreation of the wear caused by different slip angles under controlled conditions on an asphalt test track. The tyre wear was measured by collecting from the ground the rubber scrubbed off during the tests, using a specially designed filter and vacuum cleaner. Rubber was separated from the grit and dirt collected using a centrifuge before being weighed. This provided a function describing the amount of rubber worn off the tyre per unit area ( $\text{g}/\text{mm}^2$ ) for slip angles ranging from  $0^\circ$  to  $14^\circ$  at 100 kN normal load per axle. The function was used with a model of vehicle dynamics to calculate wear for complex manoeuvres.

**Keywords:** Tyre model, Tyre wear, Low emission transport, Transport operation and life cycle analysis

\*Corresponding author:

[jl974@cam.ac.uk](mailto:jl974@cam.ac.uk), Cambridge University Engineering Department, Trumpington St, Cambridge, CB2 1PZ, UK

## 1. Introduction

Heavy Goods Vehicles (HGVs) tyres are designed to achieve the best compromise between rolling resistance, skid resistance and wear. Designing tyres that are safe, fuel-efficient and long-lasting requires an in-depth understanding of the tribology of the tyre-road interaction. From an energy viewpoint, it is desirable to minimise rolling resistance, but this can only be achieved at the expense of increasing wear and stopping. Consequently, this paper is concerned with understanding tyre wear as the first step towards developing alternative optimisation strategies for HGV tyre design.

Tyre wear occurs in two different regimes: (1) when the vehicle is travelling in a straight line (friction forces primarily longitudinal) and (2) abrasive wear when cornering (friction forces primarily lateral). For HGVs with groups of unsteered rear axles, severe abrasive wear on some of the tyres when cornering due to the large slip angles caused by the geometry of the turning vehicle. Simple analytical models based only on normal pressure distribution and sliding distance covered by a tread element can represent simple tyre-wear cases but the load and slip dependence cannot be jointly described by such models (Schallamach et al. 1981). Building complete analytical models to predict tyre wear is challenging because wear depends on many factors such as the dynamics of the tyre and the vehicle, the mechanical contact conditions and tyre-road interaction, and structure of the tyre and material properties (e.g. hardness, damping, abrasion characteristics) (Wang et al. 2017; Tamada et al. 2017; Braghin et al. 2007; Huang et al. 2015). Simpler models based on fewer parameters exist, such as Silva et al. (2012)'s simplified tyre wear model and Knisley (2002)'s tread wear model which uses rolling contact friction energy, but they are based on assumptions which limit their applicability: e.g. small slip angles, fixed tyre abrasability characteristics, linear cornering stiffness, measurable contact pressure.

This paper presents a novel experimental technique to characterize tyre wear of HGVs as a function of slip angle using a semi-trailer equipped with an active steering system. Consequently the focus is on abrasive wear on cornering.

## 2. Background

The turning motion of wheeled vehicles is created by side forces acting perpendicularly to the wheels. The magnitude of the side force,  $F$ , varies as a function of the slip angle,  $\alpha$ , which is the angle between the direction of travel of the wheel (perpendicular to the centre of rotation) and the plane of the tyre. When vehicles with tandem or triaxle (or quad axle) groups negotiate small radius turns, some tyres are forced to operate at substantial slip angles (Figure 1). This causes large lateral 'scrubbing' forces and results in severe abrasive tyre wear. Scrubbing wear is strongly dependent on the tyre normal load and the radius of curvature, which is directly related to the slip angle.

For an unsteered axle group, the slip angle increases proportionally with the distance between the axle and the 'effective' axle position (Figure 1), so there is usually more severe abrasive wear on the tyres position at the extremities (first and last axle) of the group. For these tyres, the lateral abrasive wear is the principal source of in-service wear, because large braking and accelerating forces (for drive axles) causing longitudinal slip are not frequent in regular HGVs operations.

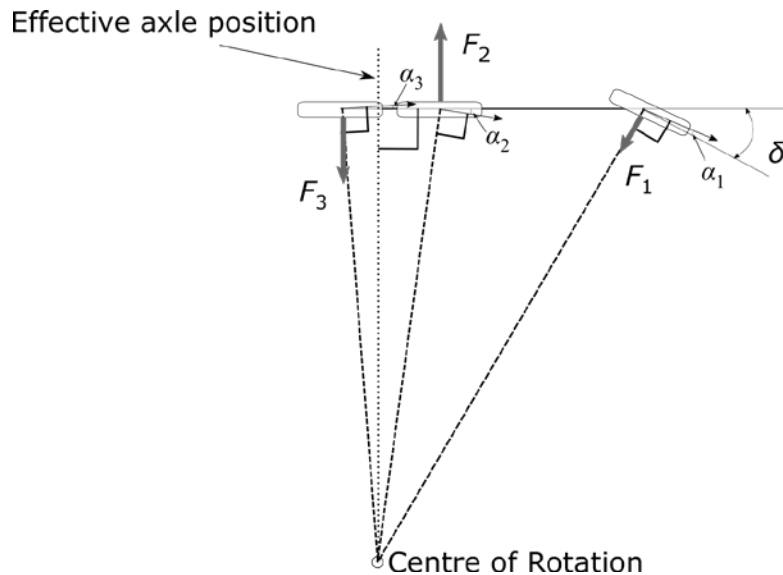


**Figure 1 – Simplified single-track model of three-axle rigid truck, showing slip angles on rear axles caused by geometry in a steady-state turn**

The relation between tyre wear, slip angles and normal load can be measured in laboratories using a tyre rotating on a (big) roller or a belt, e.g. Tire Tread Wear Simulation System from MTS Systems Corporation. It is however very challenging to recreate a realistic road surface on the roller with this type of apparatus and it recreates relatively small slip angles (max  $10^\circ$ ) and consequently mild abrasive wear, which is not the same regime as the severe abrasive wear occurring at large slip angle on the road. This means that laboratory measurements cannot be used to predict in-service wear.

### 3. Methodology

A methodology was developed to overcome this limitation using an asphalted test track and a semi-trailer with hydraulically steered axles, operating on an asphalt surface. The steerable axles enabled the vehicle to move in a straight line while maintaining a constant slip angle on the test tyres. The two rearmost axles were set to fixed steer angles of  $\pm \alpha$  opposing each other and the front trailer axle of the group was actively steered to keep the trailer moving in a straight line to ensure the tyres achieve the desired slip angle (Figure 2). Tyre wear was quantified by measuring the amount of rubber deposited on the road surface. Tests were performed over a distance shorter than the trailer wheelbase, so the tractor unit tyres did not affect the measurement.

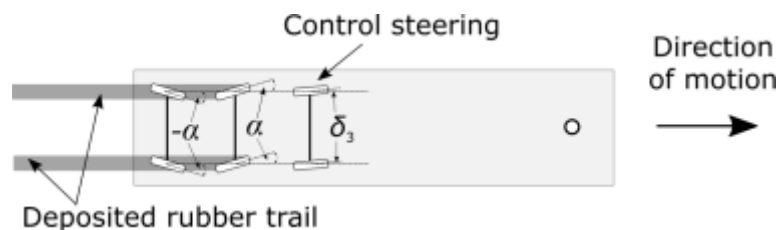


**Figure 2 – Tyre wear experimental trailer setup**

### 3.1 Experimental semi-trailer

The chassis of the trailer was manufactured by SDC Trailers Ltd (UK), and the brake system was manufactured by Haldex (Sweden). The tested tyres were Goodyear Omnitrac MST II 385/65 R22.5. Water tanks were installed inside the trailer to give a payload of 100 kN per axle (three axles, two tyres per axle). The three hydraulically-steered axles and control system were developed by TRIDEC (Netherlands). The ECU controlling each axle was programmed by the authors to maintain the two rearmost axles at fixed and opposite angles. The program also kept the semi-trailer in a straight line during the tests by controlling the front-axle steer angle proportionally to the articulation angle measured at the fifth wheel (Figure 2).

### 3.2 Data collection

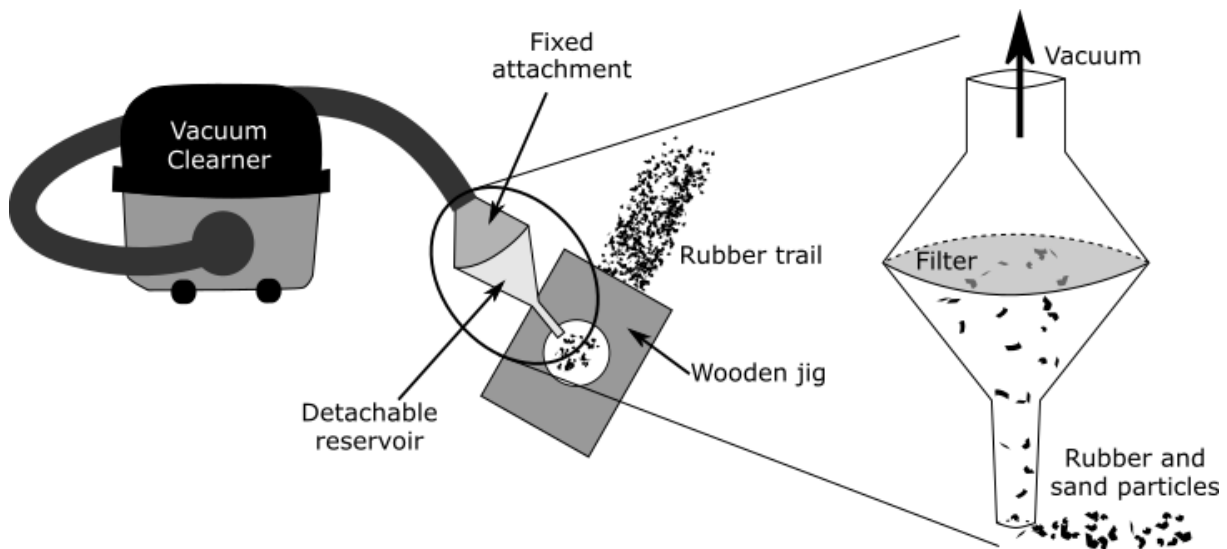


**Figure 3 – Modified vacuum cleaner to collect rubber**

The wear caused by the manoeuvre was measured by collecting the fragments of rubber deposited on a known area of the test track separating the rubber from other material such as sand and small stones, and weighing the rubber. As only a few grams of rubber per square metre was removed from the tyre during the manoeuvre, directly weighing the worn rubber was more effective than measuring the wear on the tyre (eg tread depth measurement or tyre mass comparison). A wooden jig was used to define the collection area ( $0.030 \text{ m}^2$ ) on the rubber trail left on the road surface (Figure 3). The rubber and other debris were collected using a modified vacuum cleaner end with a dedicated replaceable reservoir for each test. A 150 mm paper filter (Whatman grade 1573, pore size  $12\text{-}25 \mu\text{m}$ ) installed on each reservoir prevented rubber particles from entering the vacuum cleaner. After each test, the reservoir containing the rubber was sealed with a cork stopper.

Before each set of tests, the test track was swept to remove debris such as grit, rock, and sand. It was however almost impossible to remove all the debris from the road surface and a small quantity was collected along with the rubber particles by the vacuum cleaner. As the rubber has a lower density ( $0.9\text{-}1.2 \text{ Mg/m}^3$ ) than the other materials collected ( $2.2\text{-}3.0 \text{ Mg/m}^3$ ), it can be separated using a liquid with a density slightly higher than the rubber ( $1.8 \text{ Mg/m}^3$ ) and a centrifuge. During the centrifugal process, the greater inertial force was generated by the heavier materials, which separates them from the liquid and the rubber. The full separation of the debris took about five minutes per sample. Once separated, the rubber was dried and weighed. It was assumed that the rubber came only from the tyres on the two rearmost axles at

an equal rate since they had equal and opposite slip angles, and the front trailer axle tyres had practically no wear (ie negligible lateral and longitudinal forces). Therefore, the mass of rubber collected at each test represents the amount of rubber worn from two tyres at a certain slip angle and normal load. The mass of rubber was halved to give the wear rate for a single tyre expressed as the mass of rubber per unit area (ie g/m<sup>2</sup>).

**3.3 Experimental design**

The tyre wear measurements were performed on a short section of straight asphalt test track, with the two rearmost semi-trailer axles positioned at opposing slip angles. Tests were not performed twice on the same segment of the test track to avoid the rubber from previous tests contaminating the measurements. Tyre wear was measured at eight different slip angles between 0° and 14° with a normal load of 100 kN per axle. To avoid creating an irregular wear pattern, steering angle direction was alternated between tests – ie one test with a Counter-Clock-Wise (CCW) angle at the rear axle and Clock-Wise (CW) at middle axle and the following test with CW angle at the rear axle and CCW at the middle axle. Each measurement was repeated three times.

**3.4 Results**

Tyre wear measurements are presented in Figure 4. At this normal load, the wear measurements are best fitted with a simple quadratic function:

$$\sigma(\alpha) = K\alpha^2 \tag{1}$$

with  $K = 145 \text{ g/m}^2$ , and  $\alpha$  measured in radians (data shown in degrees at Figure 4).

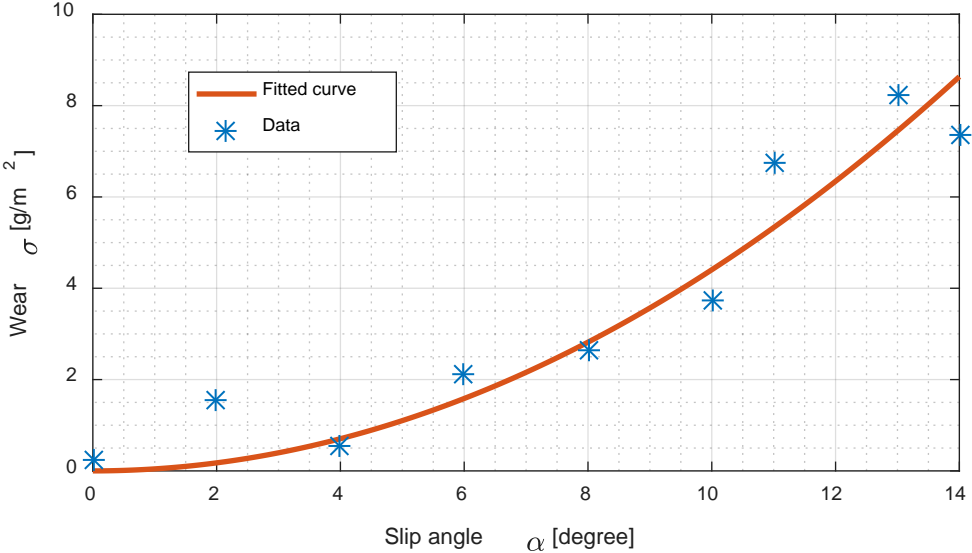


**Figure 4 – Measured tyre wear as a function of slip angle, normal load 100 kN**

**4. Tyre wear modelling**

The measured tyre wear characteristics can be used to predict the tyre wear per unit area,  $\sigma$ , as a function of slip angle,  $\alpha(s)$ , for each tyre along a given path,  $s$ .

The total mass of rubber worn from the tyre is calculated by integrating  $\sigma$  along the path:

$$\Delta M = w \int [\sigma(\alpha(s))] ds \quad (2)$$

where  $w$  is the width of the tyre.

The reduction of tread depth,  $\Delta t$ , is calculated as:

$$\Delta h = \frac{\Delta M}{d\pi w\rho} \quad (3)$$

where  $d$  is the tyre diameter ( $\Delta t \ll d$ ) and  $\rho$  is the density of the rubber.

#### 4.1 Wear estimation

The slip angles of semi-trailer axles travelling through a roundabout of different diameters (6, 12, 18 and 24 m) and exit points (90°, 180° and 270°; Figure 5) was calculated with a four-degree-of-freedom vehicle model (Figure 6). The vehicle was assumed to have a constant longitudinal speed of 5 km/h and the normal loads of the trailer axles were assumed to be 100 kN each. The steering angle of the vehicle was assumed to follow the path shown in Figure 5 and the following axles tracked off path as calculated by the simulation. Details of the model are provided in the Appendix. Examples of the typical slip angles for a 270°, 12 m diameter roundabout are shown in Figure 7.

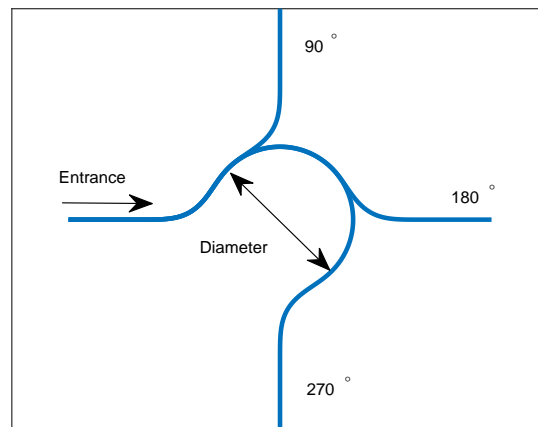


Figure 5 – Roundabout simulations for different diameters and exit points

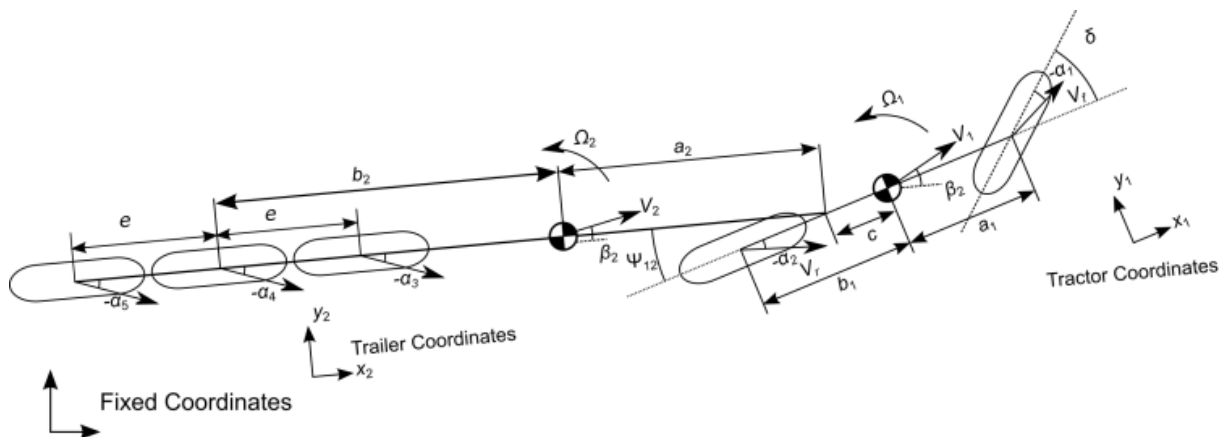
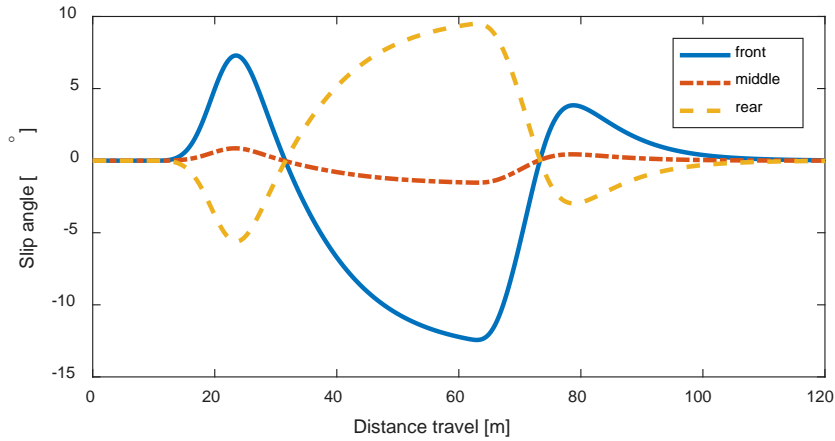
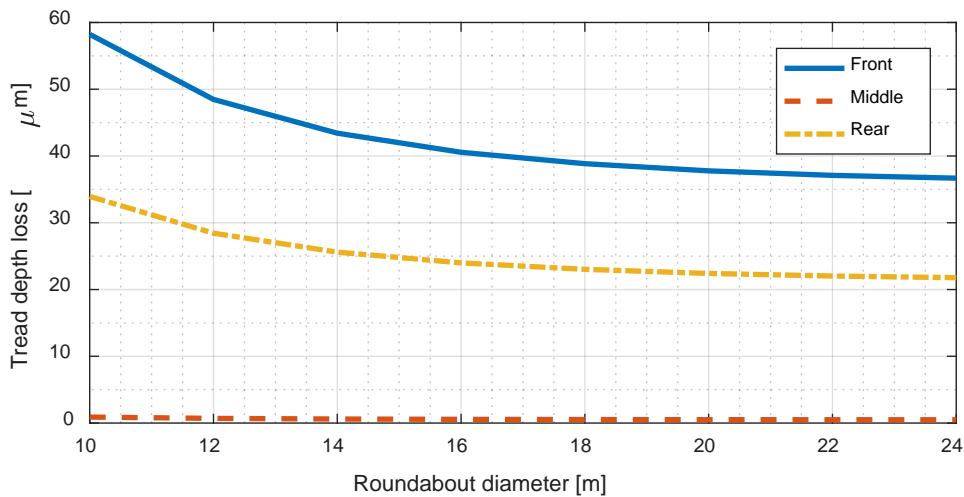


Figure 6 – Semi-trailer 'bicycle' model



**Figure 7 – Typical slip angles of a semi-trailer rear wheel for a 270° 12 m roundabout**

The tyre wear at different axle positions is shown in Figure 8 for 270° roundabouts of 10 m to 24 m diameter. The front axle of the semi-trailer has the most wear followed by the rear axle. This is because the front axle typically has the largest magnitude of slip angle. The tread depth loss in micrometer ( $\mu\text{m}$ ) at the front axle for each simulated manoeuvre is shown in Figure 9. For 90° and 180° exit angles, the wear increases with the roundabout diameter, but the opposite trend is observed for a 270° exit angle. This is because for 270° exit case, the maximum slip angle significantly decreases with the roundabout diameter. For the lower exit angle cases, the maximum slip angles do not significantly vary with the roundabout diameter, so the wear increases with the diameter because the vehicle is turning for a longer distance.



**Figure 8 – Tread depth loss for all three axles for 270° roundabouts of different diameters**

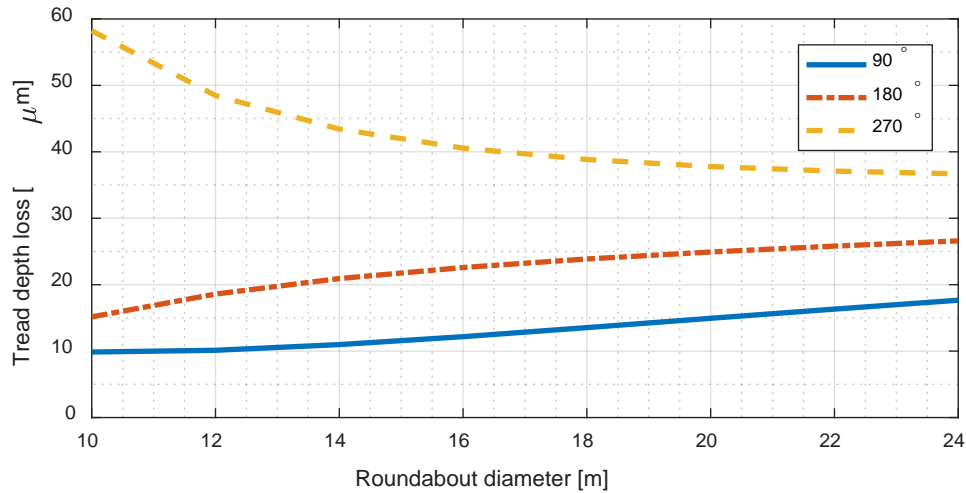


**Figure 9 – Tread depth loss at the front axle for different roundabouts**

## 5. Discussion

The empirical and large-scale tyre wear model presented in this paper enables estimation of abrasive wear due to tyre slip without the need for a complex mathematical model of wear mechanics. It also avoids many of the limitations of simplified models, e.g. limited to small slip angles and linear cornering stiffness. The major limitation of the approach is that it assumes the road surface to be constant, e.g. no major variations of the surface texture or friction with time, or presence of lubricants on the road such as water. Other models may be able to consider these factors, but it remains a challenge to measure and integrate them in the context of an in-service tyre wear prediction.

Despite this limitation, the presented tyre wear measurement method can be used for investigating low-wear tyres and the wear estimation process can be used to optimise tyre selection for vehicle fleets. Decoupling the generation of the basic wear characteristics (Figure 4) from the in-service wear prediction provides the possibility of replacing the empirical wear model with a more fundamental model of the wear process in the contact area, to give a fully analytical process during a later phase of the research.

## 6. Conclusion

The paper presented an experimental method for measuring tyre wear directly on a test track using a semi-trailer with steerable axles. Preliminary results show that for high normal load, the wear increases proportionally the square slip angle. This wear model can be used to predict in-service tyre wear. To complete this empirical tyre-wear model, the effect of normal load will be studied. The model will also be validated using in-service GPS data for the vehicle path and comparison with tread depth measurements.

## 7. References

- Schallamach, A., and K. Grosch. "Tire traction and wear." Mechanics of pneumatic tires chapter. 6, pp. 365-474, 1981.
- C. Wang, H. Huang, X. Chen, and J. Liu, "The influence of the contact features on the tyre wear in steady-state conditions," Proc. Inst. Mech. Eng. Part D J. Automob. Eng., vol. 231, no. 10, pp. 1326–1339, Sep. 2017.
- R. Tamada and M. Shiraishi, "Prediction of Uneven Tire Wear Using Wear Progress Simulation," Tire Sci. Technol. TSTCA, vol. 45, no. 2, pp. 87–100. Jun. 2017
- F. Braghin, F. Cheli, S. Melzi, and F. Resta, "Tyre Wear Model: Validation and Sensitivity Analysis," Meccanica, vol. 41, pp. 143–156, 2006.
- H. Huang, Y. Chiu, C. Wang, and X. Jin, "Three-dimensional global pattern prediction for tyre tread wear," Proc. Inst. Mech. Eng. Part D J. Automob. Eng., vol. 229, no. 2, pp. 197–213, Feb. 2015.
- M. M. Da Silva, R. H. Cunha, and A. C. Neto, "A simplified model for evaluating tire wear during conceptual design," Int. J. Automot. Technol., vol. 13, no. 6, pp. 915–922, Oct. 2012.
- S. Knisley, "A Correlation Between Rolling Tire Contact Friction Energy and Indoor Tread Wear 2 REFERENCE: Knisley, S., &quot;A Correlation Between Rolling Tire Contact Friction Energy and Indoor Tread," Tire Sci. Technol. TSTCA, vol. 30, no. 2, pp. 83–99, Apr 2002

## 8. Appendix – Vehicle model

Assumptions:

1. Longitudinal velocity of the tractor is constant ( $\dot{u} = 0$ )
2. No body roll
3. No lateral weight transfer
4. Single track vehicle

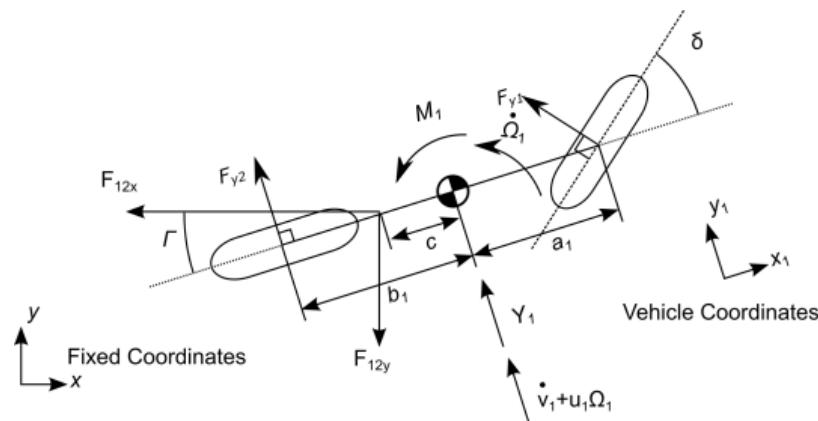


**Figure 10 – Tractor unit free body diagram**

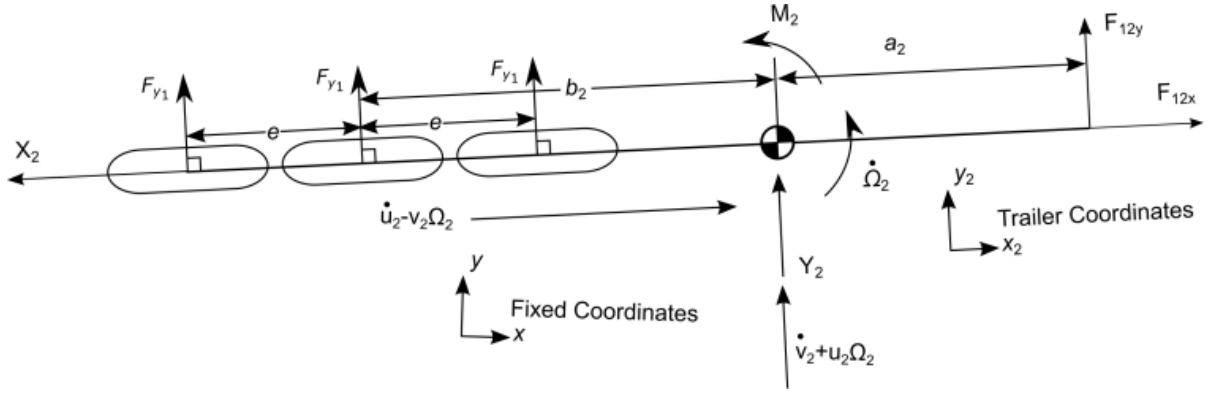


**Figure 11 – Semi-trailer free body diagram**

Definition of the velocities and accelerations

$$\Omega_2 = \Omega_1 - \dot{\Gamma} \quad (4)$$

$$u_2 = u_1 \cos(\Gamma) - (v_1 - c\Omega_1) \sin(\Gamma) \quad (5)$$

$$v_2 = u_1 \sin(\Gamma) + (v_1 - c\Omega_1) \cos(\Gamma) - a_2\Omega_2 \quad (6)$$

$$\dot{\Omega}_2 = \dot{\Omega}_1 - \ddot{\Gamma} \quad (7)$$

For  $\dot{u} = 0$ :

$$\dot{u}_2 = -(\dot{v}_1 - c\dot{\Omega}_1) \sin(\Gamma) - \dot{\Gamma}((v_1 - c\Omega_1) \cos(\Gamma) + u_1 \sin(\Gamma)) \quad (8)$$

$$\dot{v}_2 = (\dot{v}_1 - c\dot{\Omega}_1) \cos(\Gamma) + \dot{\Gamma}(u_1 \cos(\Gamma) - (v_1 - c\Omega_1) \sin(\Gamma)) - a_2\dot{\Omega}_2 \quad (9)$$

Slip angle at each tyre:

$$\alpha_1 = \arctan \frac{v_1 + a_1\Omega_1}{u_1} - \delta \quad (10)$$

$$\alpha_2 = \arctan \frac{v_1 - b_1\Omega_1}{u_1} \quad (11)$$

$$\alpha_3 = \arctan \frac{v_2 - (b_2 - e)\Omega_2}{u_2} \quad (12)$$

$$\alpha_3 = \arctan \frac{v_2 - b_2\Omega_2}{u_2} \quad (13)$$

$$\alpha_3 = \arctan \frac{v_2 - (b_2 + e)\Omega_2}{u_2} \quad (14)$$

Lateral tyre force expressed as a function of the slip angles (small angles):

$$F_{ii} = f_i(\alpha_i) = -C_i\alpha_i \quad (15)$$

Equilibrium:

$$\sum F_{y2} = -m_2(\dot{v}_2 + u_2\dot{\Omega}_2) + F_{y3} + F_{y4} + F_{y5} + F_{12y} = 0 \quad (16)$$

$$\sum F_{x2} = -m_2(\dot{u}_2 - v_2\Omega_2) + F_{12x} - X_2 = 0 \quad (17)$$

$$\sum F_{y1} = -m_1(\dot{v}_1 + u_1\Omega_1) + F_{y1} \cos(\delta) + F_{y2} + Y_1 - F_{12y} \cos(\Gamma) + F_{12x} \sin(\Gamma) = 0 \quad (18)$$

$$\sum M_{Hitch} = -I_1\dot{\Omega}_1 - m_1(\dot{v}_1 + u_1\Omega_1)c + F_{y1} \cos(\delta)(a_1 + c) - F_{y2}(b_1 - c) = 0 \quad (19)$$

$$\sum M_{Hitch} = -I_2\dot{\Omega}_2 + m_2(\dot{v}_2 + u_2\Omega_2)a_2 - F_{y3}(b_2 - e + a_2) - F_{y4}(b_2 + a_2) - F_{y5}(b_2 + e + a_2) = 0 \quad (20)$$

**Table 1 – Model constants**

Constant	Value	Unit
$u_1$	2.8	m/s
$a_1$	0.71	m
$b_1$	3.39	m
$c$	2.86	m
$m_1$	8170	kg
$I_1$	34,800	kg m <sup>2</sup>
$a_2$	6.24	m
$b_2$	1.27	m
$e$	1.65	m
$m_2$	34,000	kg
$I_2$	665,000	kg m <sup>2</sup>
$C_1$	236,000	N/rad
$C_2$	56,000	N/rad
$C_{3-5}$	83,000	N/rad